INITIAL CHARACTERIZATION OF HUMAN SPERMINE OXIDASE

A Thesis

by

PAUL RAMON JUAREZ

Submitted to the Office of Graduate Studies of
Texas A&M University
in partial fulfillment of the requirements for the degree of

MASTER OF SCIENCE

December 2008

Major Subject: Biochemistry

INITIAL CHARACTERIZATION OF HUMAN SPERMINE OXIDASE

A Thesis

by

PAUL RAMON JUAREZ

Submitted to the Office of Graduate Studies of
Texas A&M University
in partial fulfillment of the requirements for the degree of

MASTER OF SCIENCE

Approved by:

Chair of Committee,	Paul F. Fitzpatrick
Committee Members,	Dorothy Shippen
	J. Martin Scholtz
Head of Department,	Gregory D. Reinhart

December 2008

Major Subject: Biochemistry

ABSTRACT

Initial Characterization of Human Spermine Oxidase.

(December 2008)

Paul Ramon Juarez, B.S.; B.A., Texas A&M University-Corpus Christi

Chair of Advisory Committee: Dr. Paul F. Fitzpatrick

The flavoprotein spermine oxidase catalyzes the oxidation of spermine and oxygen to spermidine, 3-aminopropanol, and hydrogen peroxide. To allow mechanistic studies of the enzyme, methods have been developed to obtain large amounts of purified recombinant protein. The enzyme requires co-expression with chaperone proteins GroEL and GroES to remain soluble and active. Purification requires the use of a Ni-NTA and size exclusion column. Human spermine oxidase is a monomer with an extinction coefficient of 14000 $M^{-1}cm^{-1}$. The kinetic mechanism is ping pong. Therefore, oxygen is bound to the enzyme before spermidine is released. N1-Acetyl spermine is a slow substrate with k_{cat} and k_{cat}/K_m values 2 and 3 orders of magnitude smaller than the values for spermine. Spermidine is a competitive inhibitor, and 1,8-diaminooctane (DAO) is an uncompetitive inhibitor. The pH effects indicate that two ionizable groups are present in the k_{cat}/K_m profile and one ionizable group is in the k_{cat} profile. The reductive half reaction reveals no phase other than the reduction of the FAD, indicating the probability of a single chemical step. Reduction is not limiting to

the overall reaction. Isotope effects were determined; $^{D}k_{cat}$ at pH 7.5 = 4.1±0.4, pH 8.5 = 2.6±0.01.

DEDICATION

This thesis is dedicated to my fiancée Dianna, parents Ramon and Elva, sister Cristina, and brother Michael.

ACKNOWLEDGMENTS

I would like to thank my principal adviser, Dr. Paul F. Fitzpatrick, for his patience, guidance and support throughout this research. I would also like to thank my committee members, Dr. Shippen and Dr. Scholtz, for their guidance and friendly support throughout the course of my stay at Texas A&M University

Thanks also go to my friends and colleagues and the department faculty and staff for making my time at Texas A&M University a great experience.

Finally I would like to thank Alfredo Hernandez, Mallikarjun Lalgondar, and Cathy Cifuentes-Rojas for their relentless encouragement and friendly advice.

NOMENCLATURE

SPM	Spermine
DDAD	4,9-Dioxo-1,12-diaminododecane
DDD	1,12-Diaminododecane
DAO	1,8-Diaminooctane
FAD	Flavin adenine dinucleotide
SET	Single electron mechanism

TABLE OF CONTENTS

Page

LIST OF FIGURES

LIST OF TABLES

CHAPTER I

INTRODUCTION

Polyamines bind to DNA, RNA, proteins, and phospholipids. The positive charges interact with polyanionic macromolecules within the cells such as those on the negative phosphate backbone of DNA. Polyamine analogues alter the DNA-nuclear matrix interaction, suggesting that polyamines alter DNA structure and quite possibly function (1). Polyamine depletion can lead to the unmasking of sequences and thus reveal potential binding sites for factors regulating transcription (2).

Polyamines interact with acidic phospholipids in the membrane, possibly preventing lipid peroxidation (3, 4). Several membrane-bound enzymes such as adenylate cyclase (5), tissue transglutaminase (6), and the NMDA (N-methyl-D-aspartate), KIR (inward rectifying K^{+}) and voltage-activated Ca^{2+} channels may be regulated by polyamines (7-9). Few other compounds have as wide a regulatory role as polyamines, making polyamine metabolism both an interesting and a challenging field of study.

Intracellular polyamine concentrations are regulated by way of transport, biosynthesis, and catabolism. Polyamine export is a selective process that is regulated by the growth status of the cell (10, 11). Export is turned on by a decrease in cell growth rate and is switched back off in response to a growth stimulus (10, 11). The main

---

This thesis follows the style of *Biochemistry*.

polyamines to be exported are N1-acetyl spermidine and putrescine (11). However, spermine is the predominant intracellular polyamine; therefore, one can suggest that export is selective and that catabolism is required before efflux (12). One could also speculate that the export transporter and catabolic enzymes may share a common regulatory signal (12) (Figure 1).

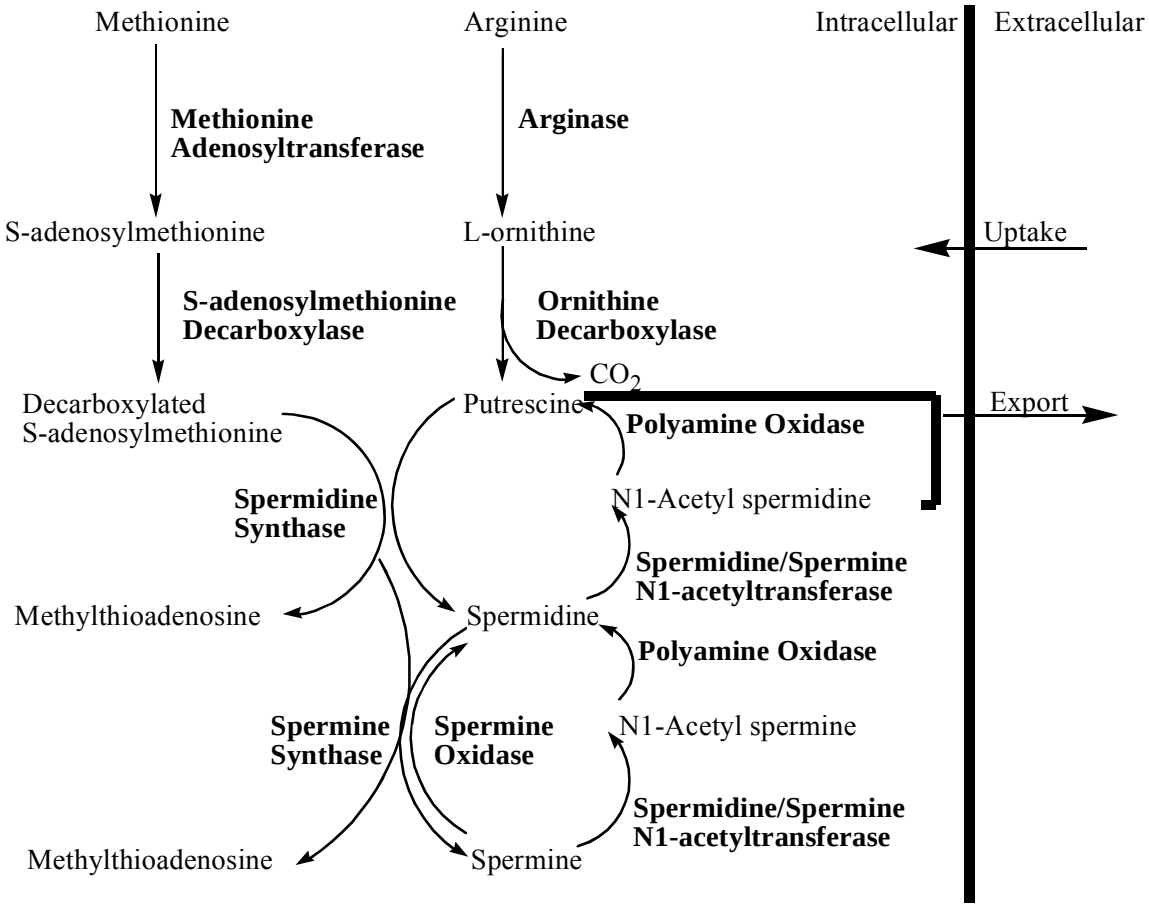

Figure 1: Polyamine metabolism.

The metabolism of the polycationic polyamines putrescine, spermidine, and spermine (Figure 1) became a target for antineoplastic therapy when they were found to be essential for normal mammalian cell growth (13). Cells have developed a very complex regulatory system for polyamines, and dysregulation can cause serious cell growth effects. Elevated levels of intracellular polyamine pools can be found in proliferative cells as well as tumor cells. Some polyamine analogues induce catabolic enzymes and thus decrease the intracellular concentration of polyamines (13). Intracellular polyamine catabolism plays an important role in polyamine homeostasis, drug response, and cell survival (13).

Initially, polyamine metabolism research focused mainly on the biosynthetic branch of polyamine metabolism. However, the newly discovered importance of the catabolic branch in homeostasis, cell survival, and drug response has led to a greater interest in the enzymes spermidine/spermine N1-acetyltransferase, polyamine oxidase, and spermine oxidase (13). In order to understand how polyamine populations are maintained one must direct more attention toward mechanistic studies of these catabolic enzymes.

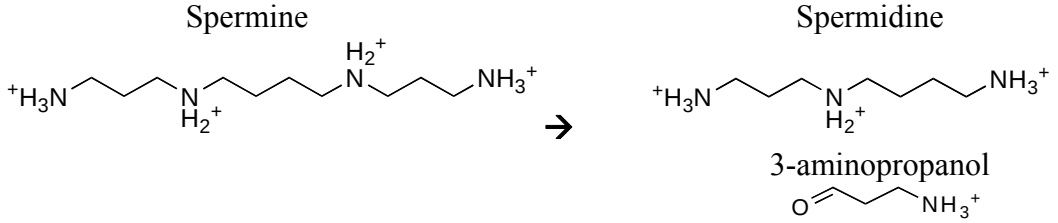

Figure 2: Oxidation of spermine by spermine oxidase at physiological pH.

Spermine oxidase is preferentially active on spermine (13-16) (Figure 2). However, Wang et al. (16) demonstrated that the recombinant human spermine oxidase can also oxidize N1-acetyl spermine. It is important to continue to identify future slow substrates which could have potential for treating cancer. Such was the case with polyamine oxidase when a slow substrate bis(ethyl)norspermine was used in phase II clinical trials for treating cancer (17).

The cytosolic protein spermine oxidase is a flavin-dependent enzyme and a member of the flavin amine oxidase family (18). Other members of this family are monoamine oxidase A and B, L-amino acid oxidase, tryptophan 2-monooxygenase, and lysine (K-specific) histone demethylase (19). Despite being implicated in a potentially cancer causing pathway, spermine oxidase has only recently been cloned (20). Its mechanism has not been determined, but spermine oxidase does have 37% sequence identity to polyamine oxidase, which could lead one to speculate that the two enzymes have similar active sites since they produce the same end product (19).

The steady state kinetic mechanism of flavin oxidases is typically divided into two half reactions (Figure 3). The first is the reductive half reaction because the bound flavin is reduced upon the bound substrate being oxidized. The second is the oxidative half reaction where the reduced flavin reacts with molecular oxygen to reoxidize the flavin and produce H_2O_2 (Figure 3).

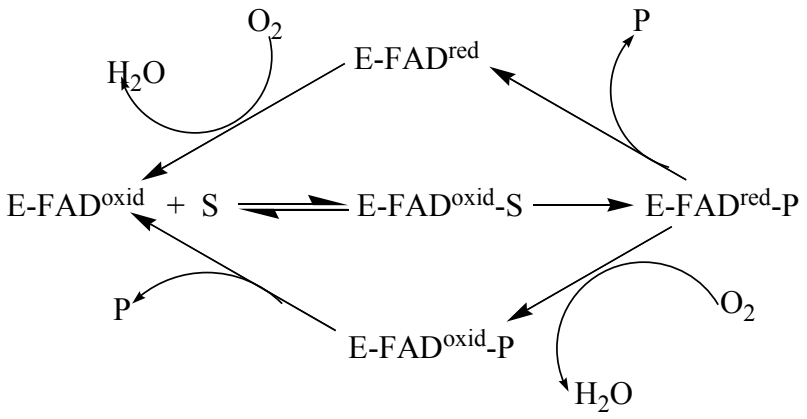

Figure 3: General catalytic reaction pathway for flavin amine oxidases.

Monoamine oxidase has served as a model enzyme for studying the mechanism of flavin amine oxidases. The enzyme has received extensive attention from the biochemical and pharmaceutical fields ever since they were found to serve as target enzymes in the treatment of depression (21). The reaction catalyzed by monoamine oxidase is the oxidative deamination of primary, secondary, and some tertiary amines. Several mechanisms have been proposed for monoamine oxidase.

A single electron transfer (SET) mechanism was proposed for monoamine oxidase based on a number of studies using cyclopropylamines as inhibitors (22-24). The mechanism begins with single electron oxidation of the substrate nitrogen to form an aminium cation radical and a flavin anionic radical. As a result of the formation of the aminium radical, the α-CH bond's pK_a is lowered, permitting proton abstraction. The next step is either a second electron transfer to the flavin semiquinone or radical recombination (forming a covalent adduct) followed by β-elimination to form the flavin hydroquinone and protonated imine products. An alternate mechanism involves the

substrate amine nucleophilically attacking the flavin at the C(4a) position, forming a flavin adduct (25). Upon formation of the adduct, the N(5) position of the flavin becomes a strong base capable of abstracting the α-hydrogen from the substrate (25).

Finally, a hydride transfer mechanism has been proposed for flavin amine oxidases (24-28). The hydride transfer mechanism involves a one-step hydride transfer from a carbon of the substrate to the flavin, directly forming the iminium product (29). No observable intermediate flavin species has been identified when the reduction of the flavin in any flavin amine oxidase is monitored with stopped flow spectroscopy, in contrast to the predictions of the SET and polar nucleophilic mechanisms (26-30). Studies with D-amino acid oxidase, N-methyltryptophan oxidase, and tryptophan 2-monooxygenase establish that the ^{15}N kinetic isotope effects are inverse due to a change in the hybridization of the nitrogen from sp^3 to sp^2 and CH bond cleavage occurring at the same time, as predicted for a hydride transfer mechanism (26-29).

Some studies of spermine oxidase have been performed using symmetrical, unsymmetrical, and conformationally restricted oligamine analogues (16). While several antitumor polyamine analogues are substrates for polyamine oxidase, none are substrates for human spermine oxidase (16, 31, 32). However, several inhibit human spermine oxidase with IC_{50} values around 100 nM (16). Human spermine oxidase is induced by some antitumor polyamine analogues (16, 33, 34). The discovery of more potent inhibitors should help determine the role of oxidase activity in polyamine homeostasis (16).

The goal of the present study is to begin a basic characterization of spermine oxidase. No group has been able to express and purify large enough quantities of spermine oxidase for mechanistic analysis. The kinetic and chemical mechanisms have not been determined. Isotope effects studies have not been conducted.

CHAPTER II

MATERIALS AND METHODS

Materials. All chemicals were purchased from Sigma-Aldrich Chemical Corp. (Milwaukee, WI), unless otherwise specified. N1-Acetyl spermine was from Fluka Chemical Co. (Milwaukee, WI). pET28b(+) was from Novagen (Madison, WI). Deuterated spermine and 4,9-dioxo-1,12-diaminododecane were synthesized by Dr. Vijay Gawandi. Human spermine oxidase cDNA plasmid pJ10:G04331 was bought from DNA 2.0. The Superdex 200HR 10/30 size exclusion column was purchased from Amersham Pharmacia Biotech AB (Uppsala, Sweden). The chaperone protein plasmids pGKJE8, pGro7, pKJE7, pGTf2, and pTf16 were purchased from Fisher Scientific.

Methods. *Construction of Expression Vector*. The human spermine oxidase gene was encoded in cDNA plasmid pJ10:G04331 by DNA 2.0. The gene was amplified via PCR with primers 5'-CTTTGTACAAGAAAGCTGGGTCATATGCA-3' and 5'-GCAGGCTGAATTCTGCGGTACCCTGTTG-3'. The PCR product and pET28b plasmid were digested with restriction enzymes *EcoRI* and *NdeI* for two hours. The digested material was run on an agarose gel and stained with ethidium bromide. Fragments of approximately 1.6 kb (PCR product) and ~5.1 kb (pET28b vector) were excised from the gel and then treated with T7 DNA ligase overnight at room temperature. The construct was used to transform competent Omnimax cells, which were plated on LB 25 μg/mL kanamycin. Plates with colonies appearing after overnight growth at 37 °C were selected and grown in 10 mL LB liquid cultures. The overnight

culture's DNA was excised and purified using a QIAprep Spin Midiprep Kit from Qiagen. The colonies were analyzed by single *(NdeI* and *EcoRI* separately) and double (*NdeI* and *EcoRI* together) restriction enzyme digests. Plasmids which showed two fragment sizes of approximately 1.6 kb and 5.1 kb on an agarose gel were further analyzed. DNA sequencing confirmed the correct sequence.

Spermine Oxidase/Chaperone Co-Expression. Five different chaperone plasmids (Table 1) were used to transform BL21DE3 cells onto chloramphenicol plates. Each plasmid contains a chloramphenicol resistance gene which allows for selection.

Table 1: Summary of chaperone plasmids and the proteins they encode.

chaperone plasmid	chaperone proteins
pGKJE8	dnaK, dnaJ, groEL, groES, grpE
pGro7	groEL, groES
pKJE7	dnaK, dnaJ, grpE
pGTf2	groEL, groES, tig
pTf16	tig

A colony from each plasmid plate was used to inoculate a tube of 4 mL of LB containing 20 μg/mL of chloramphenicol overnight. The following day, five flasks of 50 mL of LB containing chloramphenicol were inoculated with enough of the 4 mL starter cultures to bring the ratio to 1:100. The 50 mL cultures were grown to an O.D. = ~0.6. The cultures were centrifuged at 5000g for 10 minutes at 4 °C with Sorvall rotor JA14. The pellets were resuspended with 250 mL of sterile 50 mM calcium chloride and allowed to sit on ice for 25 minutes. The cells were centrifuged again then resuspended in 5 mL of

sterile 50 mM calcium chloride and 10% glycerol. They were quickly distributed to eppendorf tubes, dropped in liquid nitrogen and stored at –80 °C. The pET28SMO plasmid was used to transform the competent BL21DE3 cells containing chaperone plasmids onto kanamycin and chloramphenicol plates because the pET28b vector uses a kanamycin resistance gene for selection therefore, cells containing both the chaperone and pET plasmid can be selected for simultaneously. Colonies were picked and used to inoculate 15 mL flasks of LB containing kanamycin and chloramphenicol and allowed to shake overnight at 37 °C. A 1 mL aliquot was removed from the overnight and mixed with glycerol to a final concentration of 10% then frozen and stored in –80 °C for use as a stock for future preps. Five one liter flasks of LB containing antibiotics and the appropriate chaperone inducers L-arabinose (0.5 mg/mL) and/or tetracycline (5 ng/mL) were inoculated with 10 mL of the overnights. The large cultures' temperature was dropped from 37 °C to 18 °C when an absorbance at 600 nm of 0.2 was reached. When the absorbance reached an optical density of 0.6-0.8, the cultures were induced with a final concentration of 0.15 mM IPTG and grown for 17 hours. Cells were harvested by centrifugation at 5000g for 45 minutes at 4 °C with Sorvall 41C rotor. The cell pellet was suspended in buffer 50 mM HEPES, 10% glycerol, 2 µM pepstation, 2 µM leupeptin, 0.1 M NaCl, 100 µg/mL PMSF, and 100 µg/mL lysozyme, pH 8. Each cell paste was lysed by sonication at 30% duty and 3 cycles totaling 21 minutes (5 minutes sonication: 2 minutes rest x 3). The lysates were centrifuged at 12000g for 30 minutes at 4 °C. The clarified lysates were assayed for spermine oxidase activity.

Spermine Oxidase Purification. Cell growth was begun by streaking cells from the frozen stock containing the pET28SMO and groEL/groES chaperone plasmids onto LB kanamycin and chloramphenicol plates and incubating overnight at 37 °C. A single colony was picked and used to inoculate 70 mL LB with kanamycin and chloramphenicol. After no more than 12 hours growth at 37 °C four liters of LB with kanamycin, chloramphenicol and 0.5 mg/mL of L-arabinose were inoculated with 40 mL of the overnight. The large culture was grown at 37 °C and shaken at 250 rpm. When the absorbance at 600 nm reached ~0.2, the temperature was dropped to 18 °C. At absorbance 0.6-0.8 the large culture was induced with 0.15 mM IPTG. The cells were harvested 17 hours after induction by centrifugation at 5000g for 45 minutes at 4 °C with a Sorvall 41C rotor. The cell pellet was suspended in (5 mL buffer : 1 g cells) 50 mM HEPES, 10% glycerol, 2 μM pepstation, 2 μM leupeptin, 0.1 M NaCl, 100 μg/mL PMSF, and 100 μg/mL lysozyme, pH 8. The cell paste was lysed by sonication at 30% duty and 3 cycles for 27 minutes (7 minutes sonication : 2 minutes rest x 3).

All subsequent steps were performed at 4 °C. All centrifugations were performed for 30 minutes at 12000g using a Beckman JA14 rotor. The cell lysate was centrifuged and the pellet was discarded. While stirring, the supernatant was slowly brought to 35% ammonium sulfate then centrifuged. The 35% ammonium sulfate supernatant was brought to 50% ammonium sulfate then centrifuged. The pellet was resuspended in a minimal volume of fresh buffer 50 mM HEPES, 10% glycerol, 0.1M NaCl, 2 μM leupeptin, and 2 μM pepstatin, pH 8.

A 5 mL Ni-NTA column was equilibrated with 20 column volumes of 50 mM HEPES, 10% glycerol, 0.1M NaCl, 2 μM leupeptin, and 2 μM pepstatin, pH 8. The resuspended 50% ammonium sulfate pellet was loaded onto the column which was washed with 10 column volumes of the same buffer. The protein was eluted with a gradient of 50 mL buffer and 50 mL buffer plus 90 mM imidazole. Five mL fractions were collected, run on an SDS-PAGE gel to check for contaminating proteins, and assayed for activity. The absorbance spectrum between 300 nm and 800 nm was also examined. Fractions were pooled and concentrated by the addition of ammonium sulfate to 55% saturation and centrifuged. The pellet was resuspended in a minimal volume of 50 mM HEPES, 10% glycerol, 2 μM leupeptin, and 2 μM pepstatin, pH 8 and centrifuged again to remove small amounts of precipitate which had formed.

A Sephacel S-300 size exclusion column (3 cm x 85 cm) was equilibrated with 10 column volumes of buffer 50 mM HEPES, 10% glycerol pH 8. Approximately 6 mL of protein from the pooled Ni-NTA fractions were loaded directly onto the column and eluted with buffer. Fractions were collected, run on a gel, and assayed for spermine oxidase activity. The absorbance spectrum between 300 nm and 800 nm was also examined. Fractions were pooled and concentrated by the addition of ammonium sulfate to 55% saturation and centrifuged. The pellet was resuspended in a minimal volume of 50 mM HEPES, 10% glycerol, 2 μM leupeptin, and 2 μM pepstatin, pH 8 and centrifuged again to remove small amounts of precipitate. The protein was stored at -80 °C.

*Spermine Oxidase Extinction Coefficient***.** The absorbance of pure spermine oxidase was measured at 458 nm. A 0.8 mL sample was then denatured by the addition of 3.2 mL of 10 M urea for 30 minutes. The sample was centrifuged for 5 minutes at 12000g at 4 °C on a Beckman JA14 rotor. The absorbance of a 0.8 mL sample from the supernatant was measured again at 458 nm. The absorbance of the bound FAD was divided by the absorbance of the unbound FAD (denatured) then multiplied by the extinction coefficient of free FAD = 11,300 $M^{-1}cm^{-1}$ to calculate the extinction coefficient for the protein-FAD complex. This procedure was repeated 3 more times.

*Spermine Oxidase Molecular Weight***.** A Superdex 200 HR size exclusion column (10 mm x 30 cm) was equilibrated with 10 column volumes of 50 mM HEPES, 10% glycerol, pH 8 on an FPLC. The column was then loaded with pure spermine oxidase and standards catalase (230 kDa), tyrosine hydroxylase Δ155 (160 kDa), glucose oxidase (80 kDa), phenylalanine hydroxylase (32 kDa), and myoglobin (17 kDa). The proteins were then eluted with the same buffer.

Enzyme Assays. Enzyme activity was measured in 0.2 M Tris buffer at pH 8.5 and 25 °C by monitoring the oxygen consumption with a computer-interfaced Hansatech oxygen electrode (Hansatech Instruments) or a Yellow Springs Instrument model 5300A oxygen electrode (Yellow Springs, OH). When necessary, the oxygen concentration was varied by bubbling a sample with the desired oxygen/argon mixture. The reaction was then started by the immediate introduction of the enzyme. Rapid reaction kinetics measurements were performed with an Applied Photophysics SX-MV stopped-flow spectrophotometer. Solutions used for anaerobic experiments were made anaerobic by

first adding glucose. The solutions were cycled ten times between a vacuum and argon prior to the addition of glucose oxidase.

Data Analysis. Kinetic data were analyzed using Kaleidagraph (Adelbeck Software, Reading, PA) and Igor Pro (WaveMetrics, Inc., Lake Oswego, OR). When the concentration of one substrate was varied, Michaelis-Menten equation was fit to the initial rate data. When the concentrations of the both substrates were varied, equations 1-3 were fit to the initial rate data: equation 1 describes a sequential kinetic mechanism, equation 2 describes a ping pong mechanism, and equation 3 describes an ordered rapid equilibrium mechanism. In equations 1-3, v is the initial velocity, k_{cat} is the maximal velocity, K_a is the Michaelis constant for substrate A, and K_b is the Michaelis constant for substrate B.

$$v = k_{cat}\, AB/(K_{ia}K_b+K_aB+K_bA+AB) \quad (1)$$

$$v = k_{cat}\, AB/(K_aB+K_bA+AB) \quad (2)$$

$$v = k_{cat}\, AB/(K_aK_b+K_bA+AB) \quad (3)$$

Equations 4-6 were fit to the initial rate data from inhibition assays: equation 4 describes competitive inhibition, equation 5 describes uncompetitive inhibition, and equation 6 describes noncompetitive inhibition. In equations 4-6, [S] is the concentration of substrate, K_m is the Michaelis constant, [I] is the concentration of inhibitor, and K_i, K_{ii}, and K_{is} are inhibition constants.

$$v = (k_{cat}*[S])/([S] + K_m*(1+[I]/K_i)) \quad (4)$$

$$v = (k_{cat}*[S])/([S] + K_m*(1+K_i/[I])) \quad (5)$$

$$v = (k_{cat}*[S])/([S]*(1+[I]/K_{ii}) + K_m*(1+[I]/K_{is})) \quad (6)$$

Equations 7-8 were fit to the pH dependence of kinetic parameters: equation 7 describes the pH dependence of a kinetic parameter which decreases at high pH and equation 8 describes the pH dependence of a kinetic parameter that decreases at both high and low pH. In equations 7-8, C is the pH-independent value and K_1 and K_2 are the dissociation constants for ionizable groups.

$$\log k_{cat} = \log (C/ (1+ K_1/H)) \quad (7)$$

$$\log k_{cat}/K_m = \log (C/ (1+ K_1/H + H/ K_2)) \quad (8)$$

Equation 9 or a modified form of equation 9 was fit to the change in absorbance of the FAD with time. The rate constants for FAD reduction at different concentrations of substrate were fit to equation 10. In equations 9-10, A is the absorbance at time t, A_∞ is the final absorbance, λ is the first order rate constant, K_d is the dissociation constant and k_{red} is the limiting rate constant for flavin reduction.

$$A= A_\infty + Ae^{-\lambda t} \quad (9)$$

$$k_{obs} = k_{red}*[S] / (K_d + [S]) \quad (10)$$

Equation 11-13 were used to obtain deuterium isotope effect values; equation 11 describes isotope effects on both k_{cat} and k_{cat}/K_m, equation 12 describes an isotope effect on k_{cat} only and equation 13 describes an isotope effect on k_{cat}/K_m only. In equations 11-13, $^{D}(k_{cat}/K_m)$ is the isotope effect on k_{cat}/K_m, $^{D}(k_{cat})$ is the isotope effect on k_{cat}, and f is the fraction of the heavy atom.

$$v = (k_{cat}[S]) / (K_m(f(^{D}(k_{cat}/K_m) -1)+1)+[S](f(^{D}(k_{cat})-1)+1)) \quad (11)$$

$$v = (k_{cat}[S]) / (K_m + ([S](1+(^{D}(k_{cat})-1)f)) \quad (12)$$

$$v = (k_{cat}[S]) / (K_m + (1 + (^{D}(k_{cat}/K_m)-1)f))+[S]) \quad (13)$$

CHAPTER III

EXPRESSION AND PURIFICATION OF HUMAN SPERMINE OXIDASE

Introduction. The human isoform of spermine oxidase is studied because it has the most useful application in relation to developing medicine that can help save people's lives one day. Any results, conclusions, or findings have the potential to directly influence the development and application of human medicine used to combat cancer. Using the human isoform of spermine oxidase gives researchers in the medical and pharmaceutical fields greater confidence in this study's potential applicability as an agent in the fight against cancer.

A human spermine oxidase purification prep that can provide enough pure protein to conduct steady state and rapid reaction kinetics experiments has not yet been developed. Large amounts of pure and active protein are required for kinetic analysis. Large amounts of protein are also needed to satisfy the requirements of modern instrumentation.

Results and Discussion. *Expression Vector*. Codon usage can be a very important factor in prokaryotic gene expression. The difference in codon usage amongst species is due to the abundance of the cognate tRNAs in each species' cells. If a protein is to be expressed quickly and successfully, codons that correlate to plentiful tRNA cognates will be coded in the gene. Some proteins are expressed more slowly because it takes longer for the translation machinery to locate a rare cognate tRNA, rather than a

readily available one. This concept can be utilized to express larger quantities of a given human protein in a bacterial cell.

DNA 2.0 optimized the human spermine oxidase gene's codons for expression in *E. coli* by specifically engineering the human codons to correspond to *E. coli* codons that have an abundance of cognate tRNAs while still maintaining fidelity to the human spermine oxidase amino acid sequence. Further increases in spermine oxidase expression were attained by cloning its gene into the expression vector pET28b. The primers 5'-CTTTGTACAAGAAAGCTGGGTCATATGCA-3' and 5'-GCAGGCTGAATTCTGCGGTACCCTGTTG-3' allowed sites for NdeI (5' end) and EcoRI (3' end) to be incorporated into the ends of the PCR product. Placing the gene in pET28b can afford higher levels of protein expression therefore making it easier to purify. The plasmid has a strong lac promoter that can help drive the expression of the gene proximal to the promoter. The position of the gene within the vector also allowed a six histidine tag to be positioned at the N terminus of the protein. The histidine tag will be necessary for future protein purification steps.

Optimizing Spermine Oxidase Expression. Despite optimal conditions, proteins in unnatural environments have a tendency to form inclusion bodies. The use of tuner cells and chaperone proteins are two ways in which to keep protein from denaturing before it can be harvested. Tuner cells allow expression to be controlled depending upon the amount of IPTG added in case the protein is translated fast enough to cause the protein to aggregate. Chaperone proteins are co-expressed with the target protein and are capable of refolding the denatured protein. For example, groEL binds a denatured

protein and ATP. The binding of groES to the complex induces a conformational change allowing the denatured protein to be refolded. ATP hydrolysis allows the release of the refolded protein.

Spermine oxidase was found in inclusion bodies when initially expressed in BL21DE3 cells at 18 °C. Only 75 units per L of growth were found in the soluble form (Table 2). Tuner cells were used because their lac permease (lacY) mutation allowed a uniform entry of IPTG into the cells that created a concentration dependent and homogenous level of induction. Expression was controlled by adjusting the concentration of IPTG from lower to higher levels as seen fit. However, this method produced no more than 117 ± 4 units per liter of growth (Table 2). This was inadequate for future rapid reaction and steady state experiments. Consequentially, five different groups of chaperone proteins were used to improve the solubility of the target protein. The chaperone proteins groEL and groES produced the most units per L of growth (Table 2). Using these chaperones resulted in almost a five fold increase from ~75 (no chaperones present) units per L of growth to ~362 units per L of growth.

Table 2: Results from chaperone co-expression trials.

Chaperones	Units (μmol/minute) per L of growth
dnaK, dnaJ, groEL, groES, grpE	117 ± 11
groEL, groES	362 ± 10
dnaK, dnaJ, grpE	33 ± 4
groES, groEL, tig	96 ± 4
tig	87 ± 7
None (BL21DE3 cells)	75 ± 7
None (tuner cells)	117 ± 4

Spermine Oxidase Purification. During purification, the addition of supplemental free FAD to cell resuspension buffer was found to be unnecessary because it did not affect the spermine oxidase activity over time (Table 3). The protein was also found to be the most stable in 10% glycerol rather than 20% glycerol (Table 3).

Table 3: Spermine oxidase stability at 4 °C. Values are given in units per L of growth. Assays performed at 25 °C, pH 8.5.

Conditions	Day 0	Day 1	Day 2	Day 3	Day 7	Day 10
150 µM FAD, 10% glycerol	340±10	200±10	220±5	170±10	140±4	190±2
150 µM FAD, 20% glycerol	270±10	170±10	200±10	170±2	110±2	100±0
glycerol 10%	320±20	200±2	220±4	180±4	140±2	190±10
glycerol 20%	260±8	180±3	200±6	170±5	120±0	120±10

The purification procedure involved a Ni-NTA column and an S-300 size exclusion column. It produced 8 mg of pure protein from 54 g of cell paste (Table 4). After lysing and centrifuging the cell paste, the majority of spermine oxidase was found in the 35-50% ammonium sulfate fraction which allowed a purification of 3-fold (Table 4). The histidine tag at the N-terminus of the protein provided an opportunity to purify using a Ni-NTA column. Fractions from the Ni-NTA column were picked and pooled based on their spermine oxidase activity, purity on a gel, and spectra. All the fractions showed visible signs of contamination. Despite the contaminating factors, purification increased by 2.5 fold while maintaining 25% yield.

Table 4: Summary of the purification of spermine oxidase starting with 54 g of cell paste.

Step	Protein Conc. (mg/ mL)	Activity (Units/ mL)	Specific Activity (U/mg)	Total Units (µmol/ min)	Total mg	% Yield	Purification Fold
Clarified lysate	12.6	3.5	0.28	1000	3600	100	1.0
35-50% A.S.	15.4	14	0.93	690	750	69	3.3
Ni-NTA column	18.4	42	2.3	250	110	25	8.2
S-300 column	4.1	14	3.4	28	8.2	2.8	12

A S-300 size exclusion column was then employed to isolate spermine oxidase based on its size. No visible signs of contaminating proteins were found in the S-300 fractions so they were pooled and stored based on the same criteria used for the Ni-NTA fractions (Figure 4). The spermine oxidase band falls just above the 62 kDa molecular weight marker indicating that its molecular weight is ~65 kDa (Figure 4). The calculated molecular weight based on the DNA sequence is ~66 kDa, very close to what is seen on the SDS-PAGE gel (Figure 4). The spectrum of the pure spermine oxidase after all purification steps is characteristic of other flavoproteins such as polyamine oxidase (35) and tryptophan 2-monooxygenase (28) (Figure 5). The enzyme activity did not begin to drop until after 6 hours at room temperature (Table 5).

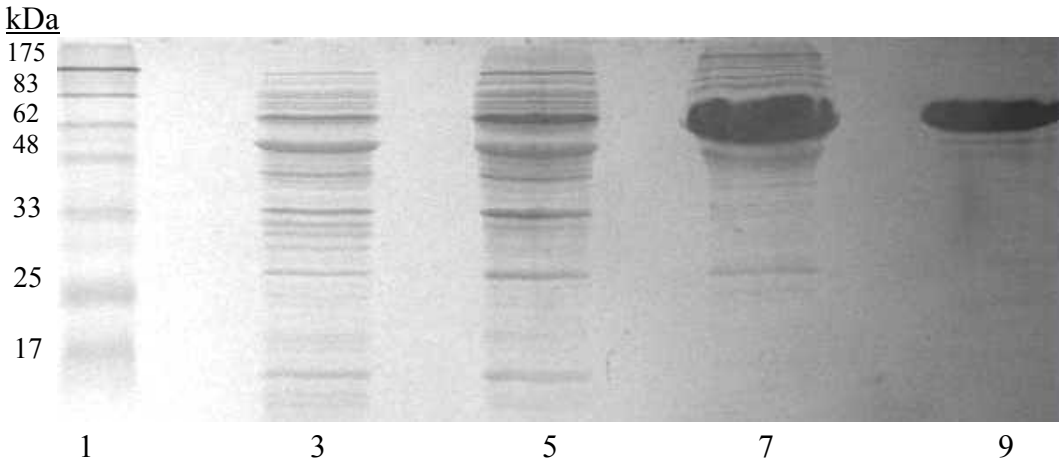

Figure 4: SDS PAGE gel of purification progress. Lanes: 1 molecular weight markers; 3 clarified lysate; 5 50% ammonium sulfate pellet; 7 Ni-NTA column; 9 S-300 column.

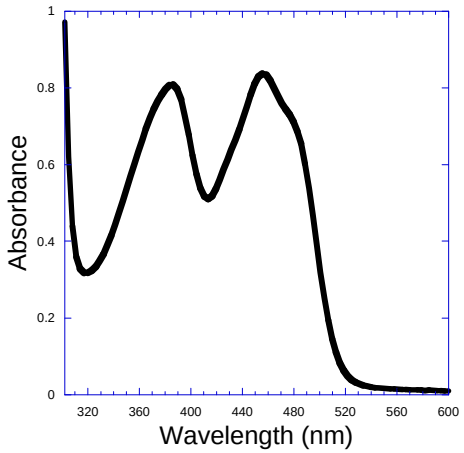

Figure 5: Final spectrum of human spermine oxidase.

Table 5: Spermine oxidase stability.

Minutes	Activity (Units/mL) Ice	Activity (Units/mL) 25 °C
0	15±1	15±1
10	15±0	15±0
20	16±0	15±1
30	17±0	15±0
60	16±0	15±0
120	16±1	15±0
240	16±0	15±1
360	15±0	14±0

Spermine Oxidase Extinction Coefficient. FAD cofactors are often exploited to determine the extinction coefficient of the protein they are bound to. The extinction coefficient can be used to determine the amount of enzyme present. In the case of spermine oxidase, the characteristic flavoprotein spectrum exhibited a peak at 458 nm (Figure 5). When the protein was denatured and devoid of its FAD cofactor the peak at 458 nm disappeared. The extinction coefficient was calculated to be 14,000 ± 1,000 $M^{-1}cm^{-1}$ by dividing the absorbance of the folded protein at 458 nm by the absorbance of the denatured protein then multiplying by the free FAD extinction coefficient of 11,300 $M^{-1}cm^{-1}$ at 450 nm. The binding of the FAD to spermine oxidase perturbed its spectrum. The visible absorbance maximum of free FAD is at 450 nm but when FAD is bound to spermine oxidase the maximum is 458 nm. The shoulder of the 458 nm peak is representative of a FAD bound to a protein.

Spermine Oxidase Molecular Weight. The absorbance of protein eluting off the Superdex 200 HR 10/30 size exclusion column was monitored so that the molecular weight of the nondenatured enzyme could be approximated. Spermine oxidase eluted at

11.6 mL, promptly after glucose oxidase (80 kDa) eluted at 11.4 mL (Figure 6). Based on the standard curve spermine oxidase's molecular weight is ~73 kDa. This is close to what was predicted from the DNA sequence and the SDS-PAGE gel (Figure 4). Spermine oxidase is most likely a monomer.

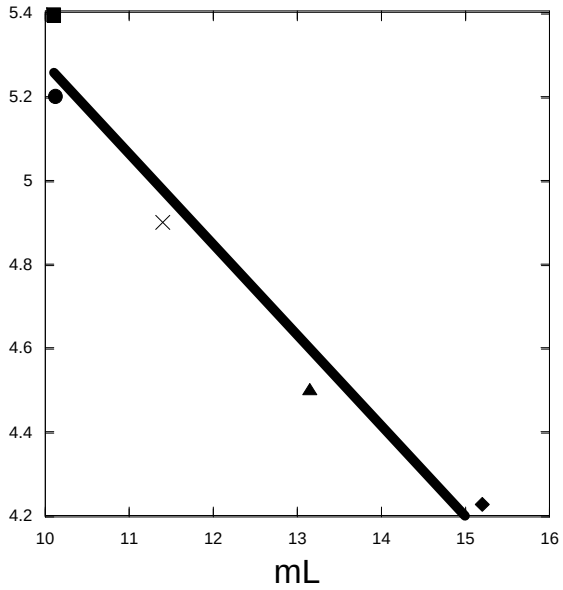

Figure 6: Gel filtration standard curve. Standards: myoglobin (υ 17 kDa), phenylalanine hydroxylase (σ 32 kDa), glucose oxidase (x 80 kDa), Δ155 (λ 160 kDa), and catalase (ν 200 kDa) fit to straight line y = 7.3 -0.21*x, $R^2 = 0.98$.

CHAPTER IV

STEADY STATE AND RAPID REACTION KINETICS

Introduction. Spermine oxidase catalyzes the reaction of spermine and oxygen to spermidine, hydrogen peroxide, and 3-aminoproponal. Its cofactor is FAD. Little is known about either its chemical or kinetic mechanism. To understand the catalytic mechanism of any enzyme, the kinetic mechanism must first be determined. The results of this analysis are diagnostic of the order of addition of substrates and the release of products and of the relative values of various microscopic rate constants (36).

Another way of characterizing the catalytic mechanism is by identifying compounds that inhibit the protein. If a potential inhibitor competes for the active site (competitive inhibition) with the substrate, the compound will most likely contain some qualities worthy of binding the active site like a substrate but not catalyzing it. Often times, the most obvious competitive inhibitor is its product because it had to have been bound to the enzyme at some point. If a slow substrate is found, the compound can be scrutinized for qualities capable of binding and catalysis but not to the magnitude of the physiological substrate.

The peak of the spermine oxidase FAD visible absorbance spectrum is located at 458 nm. The absorbance at this point would drop greatly if the protein was reduced. This is a common characteristic among flavoproteins. During this process electrons are transferred from the substrate to the flavin. If monitored anaerobically, the reduction of

spermine oxidase can be isolated and monitored at 458 nm. This would give a great insight into the rates of various steps that may exist within the reductive half reaction.

Kinetic isotope effects are a very efficient technique in identifying intermediates in enzymatic reactions. An isotopic substitution can greatly modify the reaction rate when the isotope is placed in a chemical bond that will be broken or formed in the rate limiting step. Deuterated spermine should display a primary isotope effect since it contains bonds that will be broken.

Results and Discussion. *Steady State Kinetic Mechanism.* Initial rates of oxygen consumption were measured while varying the concentrations of both oxygen and spermine. The data were fit to equations 1-3; the resulting kinetic parameters are shown in Table 6.

Table 6: Steady state kinetic parameters for spermine oxidase at pH 8.5, 25 °C.

Equation	k_{cat} (s^{-1})	K_{O2} (mM)	k_{cat}/K_{O2} (s^{-1} mM^{-1})	K_{Spm} (μM)	k_{cat}/K_{Spm} ($s^{-1}\mu M^{-1}$)	$K_{i,Spm}$ (μM)	χ^2
1	29±7	1.6±0.5	18±2	220±110	0.13±0.04	10±27	11
2	31±6	1.7±0.5	18±2	260±80	0.12±0.02	NA	11
3	21±3	0.016±0.002	22±3	22±0.08	0.14±0.05	NA	29

The fits to the sequential and ping pong mechanism are statistically the same. However, the $K_{i,Spm}$ value for the sequential mechanism is not significantly different from zero. This would suggest that the $K_{i,Spm}$ is actually equal to zero and the ping pong mechanism is correct. This finding is in good agreement with what was found in other

flavin amine oxidases such as tryptophan 2-monooxygenase (28) and polyamine oxidase (30).

Inhibition Trials. Spermidine, 4,9-dioxo-1,12-diaminododecane (DDAD), 1,12-diaminododecane (DDD), 1,8-diaminooctane (DAO), and N1-acetyl spermine are all analogs of spermine and potential inhibitors (Figure 7). Concentrations up to 8 mM of DDAD and DDD failed to show any sign of activity or inhibition toward spermine oxidase.

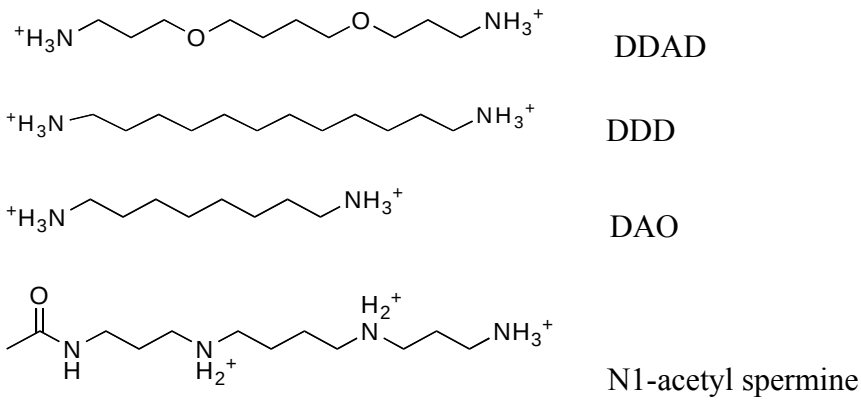

Figure 7: Possible spermine oxidase inhibitors.

N1-Acetyl spermine is a substrate of spermine oxidase. The parameters k_{cat}^{app} and k_{cat}/K_m of N1-acetyl spermine differed from spermine by three orders of magnitude (Table 7). The slow catalysis may be attributed to the acetyl group on one end of the compound creating a less than favorable orientation (with respect to spermine) within the active site.

Table 7: The apparent steady state parameters of spermine versus N1-acetyl spermine at pH 8.5, 25 °C.

Substrate	k_{cat}^{app} (s^{-1})	k_{cat}/K_m (s^{-1} mM^{-1})	K_m^{app} (μM)
Spermine	11±0.4	148±18	74±11
N1-acetyl spermine	0.15±0.006	0.73±0.08	210±30

Spermidine and DAO do not show sign of activity with spermine oxidase but were examined as inhibitors versus spermine (Table 8 and Table 9). Judging from the χ^2 value, uncompetitive inhibition for spermidine is not a good fit (equation 5, Table 8). Noncompetitive inhibition is statistically a good fit, but the K_{is} value is not significantly different from zero. Therefore this equation would not be a logical choice for spermidine inhibition (equation 6, Table 8). Competitive inhibition is the most likely form of inhibition. Spermidine is a product of spermine oxidase so it comes as no surprise that it is also a competitive inhibitor (Figure 2).

Table 8: Summary of fits to inhibition equations using spermidine.

Equation	K_{is} (mM)	K_{ii} (mM)	χ^2
4	1.2±0.2	NA	11
5	NA	0.17±0.3	78
6	1.3±0.5	23±130	1

Table 9: Summary of fits to inhibition equations using DAO.

Equation	K_{is}(mM)	K_{ii} (mM)	χ^2
4	0.39±0.46	NA	4
5	NA	12±1.8	3
6	2.0±1.0	24±5.7	1

The K_{ii} and K_{is} values for DAO in equations 5 and 6 are very high so even if they are good fits it would not be a useful inhibitor (Table 9). DAO is most likely a noncompetitive inhibitor since this is its best fit (Table 9).

pH Effects. The effect of pH on the kinetics of spermine was determined. The apparent k_{cat}^{app} pH profile reveals the involvement of one ionizable group needing to be protonated for activity with an apparent pK_a value of 9.9 ± 0.1 (Figure 8). The $k_{cat}/K_{spermine}^{app}$ pH profile is bell shaped indicating involvement of two ionizable groups with one requiring deprotonation and the other requiring protonation for activity (Figure 8). The two pK_a values are too close together to resolve, but have an average value of 8.7 ± 0.1. The ionizable groups that affect k_{cat}^{app} and $k_{cat}/K_{spermine}^{app}$ pH profiles might be attributed to the primary and secondary amine groups of spermine.

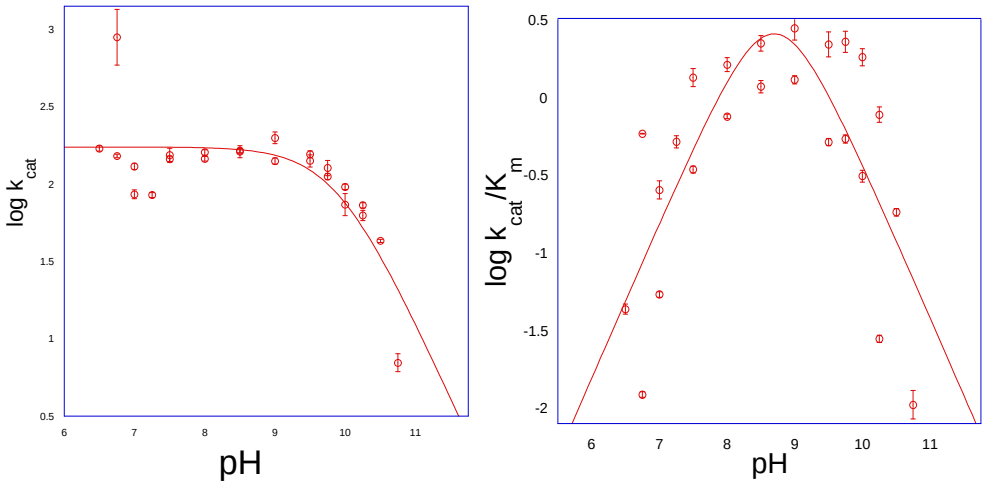

Figure 8: pH profile for spermine oxidation by spermine oxidase. The k_{cat} and $k_{cat}/K_{spermine}$ pH profiles were fit to equations 7 and 8.

Spermine contains four nitrogen groups which would make it difficult to discern the true culprits of the pH dependence since their pK_a values range from 8 to 11 (34). The pK_a on the left side of the bell shaped $k_{cat}/K_{spermine}$ pH profile is not present in the k_{cat} pH profile so it is likely to be involved in binding. Therefore, there is an ionizable group that requires protonation for binding. Reactive substrate nitrogen(s) for monoamine oxidase and maize polyamine oxidase have been suggested to require deprotonation for binding (37, 38).

Reductive Half Reaction. Single wavelength anaerobic stopped flow spectroscopy was used to determine the rate of reduction of the FAD-bound protein by its substrate spermine. Different concentrations of spermine were reacted with spermine oxidase and monitored over time at 458 nm. The traces were then fit to equation 9. The observed rate constants from each trace were then fit to equation 10 to reveal a limiting rate constant of reduction equal to $57 \pm 2.5\ s^{-1}$ and a K_d value of $17 \pm 6\ \mu M$ (Figure 9).

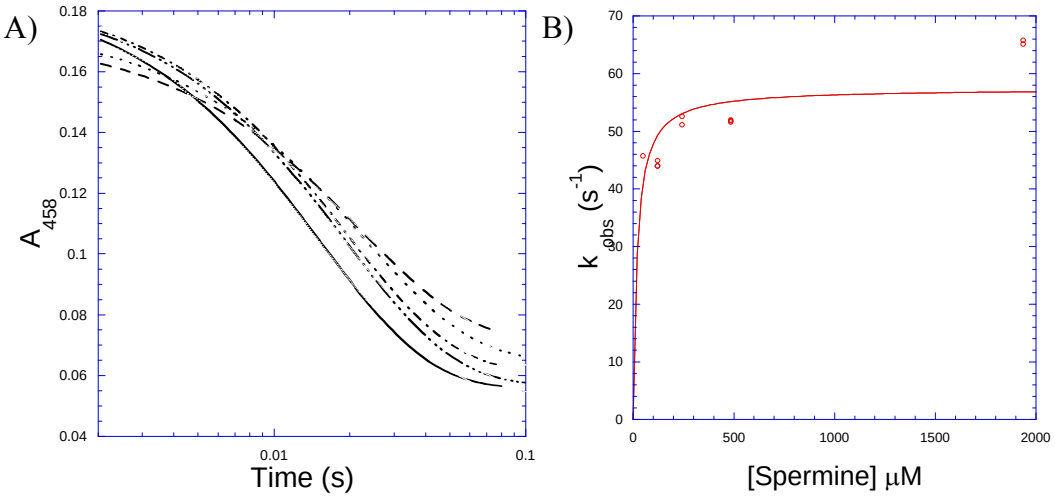

Figure 9: Reductive half reaction for spermine oxidase. (A) Traces monitored at 458 nm over time at different concentrations of spermine: 50 µM (----), 120 µM (••••), 240 µM (•-•-), 480 µM (-•••-•••), and 1.9 mM (——) (B) Observed rate constants from graph A versus the concentration of spermine.

The rate constant of reduction is two times higher than the steady state k_{cat} (s^{-1}) suggesting that the rate of reduction is not limiting for the reaction (Table 6). The reductive half reaction traces of spermine oxidase suggest that spermine is oxidized by a hydride transfer (Figure 9). No other phases are seen as the FAD is reduced therefore no detectable intermediates are present suggesting that the mechanisms proposed for monoamine oxidase are not applicable for spermine oxidase.

Deuterium Isotope Effects. Deuterated spermine was used to identify isotope effects on k_{cat}^{app} (s^{-1}) and k_{cat}/K_m^{app} (s^{-1} μM^{-1}) (Table 10). Statistically, equation 11 and 12 are the better fits than equation 13 (Table 10). The $^{D}k_{cat}/K_m$ values in equation 11 are very close to one meaning there is probably no isotope effect on $^{D}k_{cat}/K_m$ and equation 12 gives the best fit (Table 10). Equation 12 shows isotope effects on $^{D}k_{cat}$ between 2.6

and 4.8 at pH 7.5-8.5. Since the $^{D}k_{cat}/K_m$ value is one, the rate constant for catalysis is much faster than the rate of dissociation of the enzyme-substrate complex, i.e., spermine is a sticky substrate. Furthermore, the isotope effect on $^{D}k_{cat}$ increases at non-optimal pH levels indicating that the values are not the intrinsic isotope effects.

Table 10: Summary of isotope effects fit to equations 11-13.

pH	Equation	$^{D}k_{cat}/K_m$ ($s^{-1}\ \mu M^{-1}$)	$^{D}k_{cat}{}^{app}$ (s^{-1})	χ^2
7.5	11	-1.7±1	4.8±0.5	1
	12	NA	4.1±0.4	1
	13	43±20	NA	6
8.5	11	1.0±0.5	2.6±0.1	1
	12	NA	2.6±0.01	1
	13	37±20	NA	13
9.5	11	0.55±0.4	3.1±0.2	1
	12	NA	3.0±0.2	1
	13	17±7	NA	8

Intrinsic isotope effects can be masked by slow chemical steps, before or after the isotope sensitive step, slow product release, and a tendency of substrates to commit to catalysis rather than remain in equilibrium with the solution. These factors can sometimes be reduced when assays are performed at pH levels that are not the enzyme's optimum (39). In the case of spermine oxidase, the primary deuterium isotope effects are slightly higher at pH 7.5 and 9.5 and lowest at spermine oxidase's pH optimum 8.5. This could be an early indication of commitment factors or a slow chemical step masking the intrinsic isotope effects.

CHAPTER V

CONCLUSIONS

The studies presented here have focused on the expression, purification and initial characterization of human spermine oxidase. Chapter III demonstrated that the chaperone proteins groEL and groES had to be coexpressed with spermine oxidase to prevent it from forming inclusion bodies. It was not surprising that human spermine oxidase formed inclusion bodies because it was being translated in a foreign environment (*E. coli* cell). Other groups have tried to purify human spermine oxidase by renaturing it via dialysis (16). However, their overall yield is insufficient for rapid reaction kinetics. Once the protein was expressed in large enough quantities using groEL and groES, it was purified with a Ni-NTA and a size exclusion column. The Ni-NTA column is usually very reliable in that it purifies histidine tagged proteins with exceptional cleanliness even when the tag is buried, but in the case of human spermine oxidase contaminants were still visible. The S-300 size exclusion column was able to yield enough pure spermine oxidase to allow steady state and rapid reaction kinetics studies to begin. A higher yield of protein might have been attained if a smaller S-300 column had been used. However, this might have also increased the chances of including contaminating proteins that may be close in size to spermine oxidase. This study would mark the first time human spermine oxidase has been expressed and purified in large enough quantities to be able to pursue these studies. Spermine oxidase is also ready to be sent to our collaborator Dr. Allen M. Orville for crystal trials.

Chapter IV focused on characterizing the kinetic parameters of spermine oxidase. Spermine oxidase catabolizes spermine and oxygen to spermidine, hydrogen peroxide and 3-aminopropanol. The steady state kinetic parameters were determined; the kinetic mechanism is ping pong. This study has reported the first proposal for the kinetic mechanism of spermine oxidase. A ping pong kinetic mechanism is consistent with what has been reported for other flavin amine oxidases such as D-amino acid oxidase, tryptophan 2-monooxygenase, and polyamine oxidase (26-30).

N1-Acetyl spermine is a very slow substrate. The acetyl group is bulky and may have perturbed the orientation of the spermine moiety within the active site. This finding could be followed in future studies by examining other spermine-based substrates that contain smaller or bulkier groups than an acetyl group.

Spermidine is a competitive inhibitor versus spermine which indicates that 8 carbon chains with amino groups on each end and in the four carbon position can be bound to the enzyme. Spermidine is a product of spermine oxidase so it was not surprising to find out it was also a competitive inhibitor. A pH profile of the K_i values (pK_i vs. pH) of spermidine could be compared to the k_{cat}/K_m profile, since spermidine binds to the free form of the enzyme competing with the substrate for the active site.

DAO is a weak noncompetitive inhibitor, with a K_{is} value close to the K_{is} value for spermidine. DAO could also be capable of binding to an enzyme-substrate complex as well as free enzyme, making it a noncompetitive inhibitor.

The pH effects for spermine oxidase show one ionizable group in the k_{cat} profile and two ionizable groups in the k_{cat}/K_m profile, suggesting that the protonation state of

two groups may be critical for binding. Potential ionizable groups include the amino groups of spermine which have pK_as near the pK_as for the k_{cat} and k_{cat}/K_m profiles. At physiological pH spermine is fully protonated, but at pH 8.5 spermine is triply protonated (40). This would leave one unprotonated group that could be what the k_{cat}/K_m profile is identifying on the left side of the bell shaped curve. The protonated groups that both the k_{cat} and k_{cat}/K_m profiles describe could be one of the three protonated groups on spermine. In this case, a crystal structure of spermine oxidase would be very helpful in understanding the intricacies of the enzyme active site and the ionizable groups that may play a part in binding and/or catalysis.

The pre-steady state rapid reaction kinetics of the reductive half reaction of spermidine oxidase show only one visible phase, suggestive of a single phase for reduction such as a hydride transfer. This discovery directly contradicts the expectations of the SET and polar nucleophilic attack chemical mechanisms. Both predict multiple phases within the reductive half reaction. A limiting rate constant for reduction two times higher than the steady state k_{cat} indicated reduction is not limiting. This was not a surprising find since spermine is spermine oxidase's preferential substrate. Further tests with a slow substrate could make chemical steps rate limiting and allow intrinsic rate constants, isotope effects, and pK_a values to be measured. The oxidative half reaction can also be examined. The reductive half reaction's absorbance change seemed to end at ~0.1 seconds (Figure 9). At that time, an oxygen solution can be added to the mix and the reaction monitored spectroscopically.

Deuterium isotope effects on k_{cat}^{app} over the pH range 7.5-9.5 were determined. The isotope effects at pH 7.5 and 9.5 were larger than at the pH optimum 8.5. This would indicate the involvement of commitment factors masking the intrinsic rate constants. The k_{cat}/K_m value consists of rate constants from the binding step to the first irreversible step while the k_{cat} value consists of rate constants from the first irreversible step to product release. There is an isotope effect on $^{D}k_{cat}$ but not on the $^{D}k_{cat}/K_m$ value, which suggests that the substrate spermine is sticky. That means that the substrate reacts much faster than it dissociates from the enzyme-substrate complex. Intrinsic isotope effects are always pH independent, which suggests that these values are not the intrinsic isotope effects.

Future studies can find the intrinsic rate constants by using a non-optimal pH level for catalysis as well as using a slower substrate. This would allow the analysis to focus on the rate limiting or isotope sensitive step. ^{15}N effects would also divulge valuable information concerning the amino group where the carbon-hydrogen breaking occurs. If the ^{15}N kinetic isotope effects are inverse due to the change in hybridization of a nitrogen group on spermine from sp^3 to sp^2 occurring at the same time as carbon-hydrogen bond breaking; the data would suggest that the labeled nitrogen group is involved in the chemical reaction.

REFERENCES

1. Basu, H. S., Wright, W. D., Deen, D. F., Roti-Roti, J., and Marton, L. J. (1993) Treatment with a polyamine analog alters DNA matrix association in HeLa cell nuclei: a nucleoid halo assay, *Biochemistry 32*, 4073-4076.

2. Morgan, J. E., Blankenship, J. W., and Matthews, H. R. (1987) Polyamines and acetopolyamines increase the stability and alter the conformation of nucleosome core particles, *Biochemistry 26*, 3643-3649.

3. Schuber, F. (1989) Influence of polyamines on membrane function, *Biochem J. 260*, 1-10.

4. Tadolini, B. (1988) Polyamine inhibition of lipoperoxidation. The influence of polyamines on iron oxidation in the presence of compounds mimicking phospholipid polar heads, *Biochem. J. 249*, 33-36.

5. Wright, R. K., Buehler, B. A., Schott, S. N., and Rennert, O. M. (1978) Spermine and spermidine, modulators of the cell surface enzyme adenylate cyclase, *Pediatr. Res. 12*, 830-833.

6. Beninati, S., Gentile, V., Caraglia, M., Lentini, A., Tagliaferri, P., and Abbruzzese, A. (1998) Tissue transglutaminase expression affects hypusine metabolism in BALB/c 3T3 cells, *FEBS Lett. 437*, 34-38.

7. Johnson, T. D. (1996) Modulation of channel function by polyamines, *Trends Pharmacol. Sci. 17*, 22-27.

8. Nichols, C. G., and Lopatin, A. N. (1997) Inward rectifier potassium channels, *Annu. Rev. Physiol. 59*, 171-191.

9. Williams, K. (1997) Interactions of polyamines with ion channels, *Biochem. J. 325*, 289-297.

10. Wallace, H. M., and Keir, H. M. (1981) Uptake and excretion of polyamines from baby hamster kidney cells (BHK-21/C13). The effect of serum on confluent cell cultures, *Biochim. Biophys. Acta 676*, 25-30.

11. Wallace, H. M., and Mackarel, A. J. (1998) Regulation of polyamine acetylation and efflux in human cancer cells, *Biochem. Soc. Trans. 26*, 571-575.

12. Wallace, H. M., Fraser, A. V., and Hughes, A. (2003) A perspective of polyamine metabolism, *Biochem J. 376*, 1-14.

13. Bellelli, A., Cavallo, S., Nicolini, L., Cervelli, M., Bianchi, M., Mariottini, P., Zelli, M., and Federico, R. (2004) Mouse spermine oxidase: a model of the catalytic cycle and its inhibition by N,N1-bis(2,3-butadienyl)-1,4-butadiamine, *Biochem. Biophys. Res. Commun*. *322*, 1-8.

14. Cervelli, M., Polticelli, F., Federico, R., and Mariottini, P. (2003) Heterologous expression and characterization of mouse polyamine oxidase, *J. Biol. Chem*. *278*, 5271-5276.

15. Vujcic, S., Diegelman, P., Bacchi, C. J., Kramer, D. L., and Porter, C. W. (2002) Identification and characterization of novel flavin-containing spermine oxidase of mammalian cell origin, *Biochem. J*. *367*, 665-675.

16. Wang, Y., Murrary-Stewart, T., Devereux,W., Hacker, A., Frydman, B., Woster, P. M., and Casero, Jr., R. A. (2003) Properties of purified recombinant human polyamine oxidase, PAOh1/SMO, *Biochem. Biophys. Res. Commun*. *304*, 605-611.

17. Bergeron, R. J., Mueller, R., Busseniu, J., McManis, J. S., Merriman, R. L., Smith, R. E., Hua, Y., and Weimar, W. R. (2000) Synthesis and evaluation of hydroxylated polyamine analogues as antiproliferatives, *J. Med. Chem*. *43*, 224-235.

18. Babbar, N., Murray-Stewart, T., and Casero Jr., R. A. (2007) Inflammation and polyamine catabolism: the good, the bad and the ugly, *Biochem. Soc. Trans. 35*, 300-304.

19. Wu, T., Yankovskaya, V., and McIntire, W. S. (2003) Cloning, sequencing, and heterologous expression of murine peroxisomal flavoprotein, N1-acetylated polyamine oxidase, *J. Biol. Chem*. *278*, 20514-22052.

20. Wang, Y., Devereux, W., Woster, P. M., Murray-Stewart, T., Hacker, A., and Casero Jr., R. A. (2001) Cloning and characterization of a human polyamine oxidase that is inducible by polyamine analogue pressure, *Cancer Res*. *61*, 5370-5373.

21. Edmondson, D.E., Mattevi, A., Binda, C., Li, M., and Hubalek, F. (2004) Structure and mechanism of monoamine oxidase, *Curr. Med. Chem*. *11*, 1983-1993.

22. Jonsson, T., Edmondson, D. E., and Klinman, J. P. (1994) Hydrogen tunneling in the flavoenzyme monoamine oxidase B, *Biochemistry 33*, 14871.

23. Silverman, R. (1992) Electron transfer chemistry of monoamine oxidase, *Adv. Elec. Tran. Chem. 2*, 177-213.

24. Silverman, R. (1995) Radical ideas about monoamine oxidase, *Acc. Chem. Res. 28*, 335-342.

25. Miller, J. R., and Edmondson, D. E. (1999) Structure-activity relationships in the oxidation of para-substituted benzylamine analogues by recombinant human liver monoamine oxidase A, *Biochemistry 38*, 13670-13683.

26. Denu, J. M., and Fitzpatrick, P. F. (1994) Intrinsic primary, secondary, and solvent kinetic isotope effects on the reductive half-reaction of D-amino acid oxidase: evidence against a concerted mechanism, *Biochemistry 33*, 4001-4007.

27. Ralph, E. C., and Fitzpatrick, P. F. (2005) pH and kinetic isotope effects on sarcosine oxidation by N-methyltryptophan oxidase, *Biochemistry 44*, 3074-3081.

28. Ralph, E. C., Anderson, M. A., Cleland, W. W., and Fitzpatrick, P. F. (2006) Mechanistic studies of the flavoenzyme tryptophan 2-monooxygenase: deuterium and 15N Kinetic isotope effects on alanine oxidation by an L-amino acid oxidase, *Biochemistry 45*, 15844-15852.

29. Ralph, E. C., Hirschi, J. S., Anderson, M. A., Cleland, W. W., Singleton, D. A., and Fitzpatrick, P. F. (2007) Insights into the mechanism of flavoprotein-catalyzed amine oxidation from nitrogen isotope effect on the reaction of N-methyltryptophan oxidase, *Biochemistry 46*, 7655-7664.

30. Royo, M., and Fitzpatrick, P.F. (2002) Mechanistic studies of mouse polyamine oxidase with N1,N12-bisethylspermine as a substrate, *Biochemistry 44*, 7079-7084.

31. Lawson, K. R., Marek, S., Linehan, J. A., Woster, P. M., Casero Jr., R. A. (2002) Detoxification of the polyamine analogue N1-ethyl-N11-[(cycloheptyl)methyl]-4,8-diazaundecane (CHENSpm) by polyamine oxidase, *Clin. Cancer Res. 8*, 1241-1247.

32. Seiler, N., Duranton, B., Vincent, F., Gosse, F., Renault, J., and Raul, F. (2000) Inhibition of polyamine oxidase enhances the cytotoxicity of polyamine oxidase substrates: a model study with N1-(N-octanesulfonyl)spermine and human colon cancer cell, *Int., J. Biochem. Cell. Biol. 32*, 703-716.

33. Devereux, W., Wang, Y., Murray-Stewart, T., Hacker, A., and Casero Jr., R. A. (2002) Differential induction of polyamine oxidase by polyamine analogues in human lung carcinoma lines, *Proc. Am. Assoc. Cancer Res*. *43*, 963-964.

34. Vujcic, S., Liang, P., Diegelman, P., Kramer, D. L., and Porter, C. W. (2003) Genomic identification and biochemical characterization of the polyamine oxidase involved in polyamine back-conversion, *Biochem. J. 370*, 19-28.

35. Royo, M., and Fitzpatrick, P. F. (2005) Mechanistic studies of mouse polyamine oxidase with N1,N12-bisethylspermine as a substrate. *Biochemistry*. *44*, 7079-7084.

36. Cleland, W.W. (1977) Determining the chemical mechanisms of enzyme-catalyzed reactions by kinetic studies. *Adv. Enzymol. Relat. Areas Mol. Biol*. *45*, 273-388.

37. Aikens, D., Bunce, S., Onasch, F., Parker, R., III, Hurwitz, C., and Clemans, S. (1983) The interactions between nucleic acids and polyamines. II. Protonation constants and 13C-NMR chemical shift assignments of spermidine, spermine, and homologs, *Biophys. Chem*. *17*, 67-74.

38. Binda, C., Mattevi, A., and Edmondson, D. E. (2002) Structure-function relationships in flavoenzyme dependent amine oxidations: a comparison of polyamine oxidase and monoamine oxidase, *J. Biol. Chem*. *277*, 23973-23976.

39. Cook, P. F., and Cleland, W. W. (1981) Mechanistic deductions from isotope effects in multireactant enzyme mechanisms, *Biochemistry 20*, 1790-1796.

40. Frassineti, C., Ghelli, S. Gans, P., Sabatini, A., Moruzzi, M. S., and Vacca, A. (1995) Nuclear magnetic resonance as a tool for determining protonation constants of natural polyprotic bases in solution, *Anal. Biochem*. *231*, 374-382.

VITA

Name: Paul Ramon Juarez

Address: Department of Biochemistry & Biophysics
103 Biochemistry/Biophysics Building
Texas A&M University
2128 TAMU
College Station, Texas 77843-2128

Email Address: pjuarez@tamu.edu

Education: B.S., Chemistry, Texas A&M University-Corpus Christi, 2005
B.A., Psychology, Texas A&M University-Corpus Christi, 2005
M.S., Biochemistry, Texas A&M University, 2008

Meetings: 2nd Annual Texas Enzyme Mechanism Conference.
University of Texas at Austin, Texas
January 5th 2008.
Poster: "Expression and Initial Characterization of Human Spermine Oxidase."
Paul R. Juarez
Dr. Paul F. Fitzpatrick PhD.